

Momentum distributions of symmetric (H_2^+) and asymmetric (HeH^{2+}) molecular ions in a circularly polarized laser field under different ionization mechanisms

Xin-Yu Hao(郝欣宇), Shu-Juan Yan(闫淑娟), Ying Guo(郭颖), and Jing Guo(郭静)

Citation: Chin. Phys. B, 2024, 33 (**12**): 123401. DOI: 10.1088/1674-1056/ad7c2b
Journal homepage: http://cpb.iphy.ac.cn; http://iopscience.iop.org/cpb

What follows is a list of articles you may be interested in

Vibronic effect study of $^1A_2$ state of H_2O and D_2O

Bei-Yuan Zhang(张倍源), Li-Han Wang(王礼涵), Jian-Hui Zhu(朱剑辉), Wei-Qing Xu(徐卫青), Zi-Ru Ma(马子茹), Xiao-Li Zhao(赵小利), Yong Wu(吴勇), and Lin-Fan Zhu(朱林繁)

Chin. Phys. B, 2024, 33 (**5**): 053401. DOI: 10.1088/1674-1056/ad24d9

Absolute partial and total ionization cross sections of carbon monoxide with electron collision from 350 eV to 8000 eV

Taj Wali Khan, Weizhe Huang(黄伟哲), Enliang Wang(王恩亮), Xu Shan(单旭), and Xiangjun Chen(陈向军)

Chin. Phys. B, 2024, 33 (**4**): 043401. DOI: 10.1088/1674-1056/ad20dd

Oscillator strength and cross section study of the valence-shell excitations of NO_2 by fast electron scattering

Qiang Sun(孙强), Jin-Feng Chen(陈锦峰), Zhi-Wei Nie(聂智伟), Jian-Hui Zhu(朱剑辉), and Lin-Fan Zhu(朱林繁)

Chin. Phys. B, 2023, 32 (**11**): 113402. DOI: 10.1088/1674-1056/acf5d6

Oscillator strength study of the excitations of valence-shell of C_2H_2 by high-resolution inelastic x-ray scattering

Qiang Sun(孙强), Ya-Wei Liu(刘亚伟), Yuan-Chen Xu(徐远琛), Li-Han Wang(王礼涵), Tian-Jun Li(李天钧), Shu-Xing Wang(汪书兴), Ke Yang(杨科), and Lin-Fan Zhu(朱林繁)

Chin. Phys. B, 2022, 31 (**5**): 053401. DOI: 10.1088/1674-1056/ac422e

Resonance enhanced electron impact excitation for P-like Cu XV

Li Shuang (李双), Yan Jun (颜君), Li Chuan-Ying (李传莹), Huang Min (黄敏), Chen Chong-Yang (陈重阳)

Chin. Phys. B, 2015, 24 (**11**): 113401. DOI: 10.1088/1674-1056/24/11/113401

Momentum distributions of symmetric (H_2^+) and asymmetric (HeH^{2+}) molecular ions in a circularly polarized laser field under different ionization mechanisms

Xin-Yu Hao(郝欣宇), Shu-Juan Yan(闫淑娟), Ying Guo(郭颖), and Jing Guo(郭静)†

Institute of Atomic and Molecular Physics, Jilin University, Changchun 130012, *China*

(Received 13 May 2024; revised manuscript received 11 September 2024; accepted manuscript online 18 September 2024)

By numerically solving the two-dimensional (2D) time-dependent Schrödinger equation (TDSE), we present photoelectron momentum distributions (PMDs) and photoelectron angular distributions (PADs) of symmetric (H_2^+) and asymmetric (HeH^{2+}) molecular ions in circularly polarized (CP) laser pulses. By adjusting the laser wavelength, two circumstances of resonance excitation and direct ionization were considered. The ionization mechanism of the resonance excitation was mainly investigated. The results show that the PMDs of H_2^+ and HeH^{2+} in the *y*-direction gradually increase with increasing intensity, and the number of PMDs lobes is in good agreement with the results predicted by the ultrafast ionization model. In the resonance excitation scenario, the PMDs of H_2^+ are dominated by two-photon ionization, whereas the PMDs of HeH^{2+} are dominated by three-photon ionization. Furthermore, the PMDs of HeH^{2+} are stronger in the resonance excitation scenario than those of H_2^+, which can be explained by the time-dependent population of electrons. In addition, the molecular structure is clearly imprinted onto the PMDs.

Keywords: resonance excitation, time-dependent Schrödinger equation, ultrafast ionization model, photoelectron momentum distributions

PACS: 34.80.Gs, 32.80.–t, 31.15.xv, 42.65.Re **DOI:** 10.1088/1674-1056/ad7c2b

1. Introduction

With the progress of science and technology, the interaction between lasers and matter produces a series of higher-order nonlinear physical phenomena, such as multi-photon ionization,[1–3] above-threshold ionization,[4,5] higher-order harmonic emission,[6–8] relativistic effects, etc.[9,10] Attosecond pulses[11,12] offer an opportunity to reveal the secrets of electron dynamics. Previously, the primary research on electron dynamics in molecules on attosecond timescales focused on linearly polarized laser pulses.[9,13] Circularly polarized (CP) laser pulses play a significant role in detecting ultrafast electron dynamics at the atomic scale because of their high temporal and spatial resolutions. CP laser pulses are currently widely employed in a variety of fields, including the production of attosecond pulses and high-order harmonics.[14–18] In intense laser fields, the momentum distribution of electrons contains information about electron dynamics.[19–21] Therefore, the photoelectron momentum distributions (PMDs) have become an effective method for studying the electron dynamics.

Meckel *et al.*[22] obtained three-dimensional (3D) PMDs of N_2 and O_2 in a linearly polarized laser field. Yuan *et al.*[23] investigated the carrier-envelope phase effects of PMDs of H_2^+ in orthogonally ultraviolet polarized laser fields. Zhang *et al.*[24] found that the PMDs of H_2^+ molecules are sensitive to nuclear distance and laser ellipticity. Li *et al.*[25] presented a systematic theoretical analysis of the electron dynamics of H_2^+, CO_2, and N_2 molecules in ultra-short linearly polarized XUV pulses, demonstrating that molecular symmetry was also imprinted onto the PMDs. Yuan *et al.*[26] investigated the effects of the ionized electron wavelength and internuclear distance on the angular distributions of H_2 and H_2^+. Moreover, the effects of molecular geometry, laser parameters, and photoelectron energy on the PMDs of H_2^+ and HeH^{2+} under intense CP extreme ultraviolet laser pulses have been investigated.[27] These results indicate that the electronic structure and symmetry of the molecule have complex effects on the PMDs when they interact with the laser field. Recent studies have shown that the excited states of atoms or molecules play a crucial role in many cases.[28,29] We propose resonance excitation as an ionization mechanism. For H_2^+, the resonance excitation from the ground state $1s\sigma_g$ to the first excited state $2p\sigma_u$ was investigated. For HeH^{2+}, the resonance excitation from the first excited state $2p\sigma$ to the second excited state $2p\pi$ was investigated. In the resonance excitation scenario, the effect of molecular symmetry or asymmetry on the momentum distribution is not clear and needs to be further explored.

In this paper, H_2^+ and HeH^{2+} are chosen for comparative investigation. HeH^{2+} is chosen because it has been widely used in experimental and theoretical studies.[30,31] The ionization of CP laser pulses on H_2^+ and HeH^{2+} ion is studied theoretically in the present work. The photoelectron distri-

†Corresponding author. E-mail: gjing@jlu.edu.cn

© 2024 Chinese Physical Society and IOP Publishing Ltd

butions of H_2^+ and HeH^{2+} in CP laser fields under different ionization mechanisms have been studied. The PMDs are obtained by solving the two-dimensional (2D) time-dependent Schrödinger equation (TDSE) and elucidated in detail by ultrafast ionization models. The structure of this paper is as follows. Section 2 describes the theoretical method. In Section 3, the PMDs and the photoelectron angular distributions (PADs) of H_2^+ and HeH^{2+} in the CP laser field under different ionization mechanisms are introduced. In Section 4, we summarize our findings. Atomic units (a.u.) $e = \hbar = m_e = 1$ are used throughout this paper unless otherwise stated.

2. Theoretical method and computational methods

We studied the ionization dynamics of symmetric (H_2^+) and asymmetric (HeH^{2+}) ions. The 2D TDSE of H_2^+ and HeH^{2+} is

$$\mathrm{i}\frac{\partial\psi(\boldsymbol{r},t)}{\partial t} = \left(-\frac{1}{2}{\nabla_{\boldsymbol{r}}}^2 + V_{\mathrm{C}}(\boldsymbol{r}) + V_{\mathrm{L}}(\boldsymbol{r})\right)\psi(\boldsymbol{r},t), \tag{1}$$

here, $-\frac{1}{2}{\nabla_{\boldsymbol{r}}}^2$ is kinetic energy of the electron, $V_{\mathrm{C}}(\boldsymbol{r})$ is Coulomb potential. The interaction between the laser field and the molecules is given by $V_{\mathrm{L}}(\boldsymbol{r}) = \boldsymbol{r}\cdot\boldsymbol{E}(t)$.

The molecular axis was oriented along the x-axis. For H_2^+ and HeH^{2+}, the expression for the soft-core Coulomb potential is as follows:

$$V_{\mathrm{C}}(\boldsymbol{r}) = -\frac{Z_1}{\sqrt{(x-R_1)^2+y^2+\alpha}} - \frac{Z_2}{\sqrt{(x-R_2)^2+y^2+\alpha}}, \tag{2}$$

where x and y are the electronic coordinates, and Z_1 and Z_2 represent the charges of the nuclei. For H_2^+, $Z_1 = Z_2 = 1$, and $R_1 = R_2 = R/2$ ($R = R_1 + R_2 = 2$ a.u.). For HeH^{2+}, $Z_1 = 2$, $Z_2 = 1$, and $R_1 = -R/5$, $R_2 = 4R/5$ ($R = R_1 + R_2 = 3.89$ a.u.).[32] Furthermore, the soft core parameter α was introduced to remove singularity. For H_2^+, $\alpha = 0.5625$. For HeH^{2+}, $\alpha = 0.5$. The ionization potentials of the $1s\sigma$, $2p\sigma$, and $2p\pi$ states of HeH^{2+} are 2.25 a.u., 1.03 a.u., and 0.74 a.u.,[33–35] respectively, whereas the $1s\sigma_g$ and $2p\sigma_u$ states of H_2^+ have ionization potentials of 1.08 a.u. and 0.65 a.u., respectively.[36,37]

The expression for the laser pulse is

$$\boldsymbol{E}(t) = \frac{1}{\sqrt{2}}E_0 f(t)[\cos(\omega t)\hat{e}_x + \sin(\omega t)\hat{e}_y], \tag{3}$$

where ω is the laser pulse's carrier frequency, and $\hat{e}_x/\hat{e}_y$ is the polarization vector. The pulse duration is $T = T_1 + T_2$, $T_1 = 20\tau$ (the number of optical periods that a laser pulse lasts), $T_2 = 10\tau$ (the number of optical periods for field-free evolution), where $\tau = 2\pi/\omega$. The pulse envelope is

$$f(t) = \begin{cases} \dfrac{t}{5\tau}, & (0 < t < 5\tau), \\ 1, & (5\tau < t < 5\tau + N), \\ -\dfrac{t}{5\tau} + \dfrac{N}{5\tau} + 2, & (5\tau + N < t < 10\tau + N), \end{cases} \tag{4}$$

where $N = 10\tau$. Through the combination of the fast Fourier transform[38,39] and the split operator approach, we are able to solve the 2D TDSE numerically

$$\psi(\boldsymbol{r},t+\Delta t) = \mathrm{e}^{-\mathrm{i}(\frac{p^2}{4})\Delta t}\,\mathrm{e}^{-\mathrm{i}[V_{\mathrm{C}}(\boldsymbol{r})-V_{\mathrm{L}}(\boldsymbol{r},t)]\Delta t}\,\mathrm{e}^{-\mathrm{i}(\frac{p^2}{4})\Delta t}\psi(\boldsymbol{r},t) + O(\Delta t)^3, \tag{5}$$

where the time step $\Delta t = 0.05$ a.u., and the total spatial length is 409.6 a.u. The space step size in the x and y directions was 0.25 a.u. During the time evolution, to suppress the unphysical effects induced by the wave packets at the boundaries, we multiply the wave function at each time step by an absorption function, with the absorption boundaries set from 150 a.u. to 204.8 a.u. $\Psi(\boldsymbol{r},t)$ represents the time-dependent wave function and the wave function of the ionized parts is $[1-M(\boldsymbol{r})]\Psi(\boldsymbol{r},t)$, where $\boldsymbol{r} = \sqrt{x^2+y^2}$,

$$M(r) = \begin{cases} 1, & r \le r_{\mathrm{b}}, \\ \exp[-\beta(r-r_{\mathrm{b}})], & r > r_{\mathrm{b}}, \end{cases} \tag{6}$$

where $\beta = 1$, and r_{b} denotes the boundary between the ionized electron wave function and bounded wave function. For both H_2^+ and HeH^{2+}, r_{b} was set as 50 a.u. The electron wave function of the ionized part can be expressed as

$$\psi_{\mathrm{i}}(x,y,t_{\mathrm{f}}) = [1-M(r_{\mathrm{b}})]\,\psi(x,y,t_{\mathrm{f}}). \tag{7}$$

By Fourier transforming the wave function of the ionized component in the coordinate space, the wave function in the momentum space can be obtained. The PMDs are then obtained by squaring it

$$D(p_x,p_y,t_{\mathrm{f}}) = \left|\frac{1}{2\pi}\iint \mathrm{d}x\mathrm{d}y\,\mathrm{e}^{-\mathrm{i}(xp_x+yp_y)}\psi_{\mathrm{i}}(x,y,t_{\mathrm{f}})\right|^2. \tag{8}$$

The PADs were derived from PMDs. Using angle statistics, the PADs can be obtained.

3. Results and discussion

In our calculations, we investigated the PMDs and PADs of symmetric H_2^+ and asymmetric HeH^{2+} molecular ions in circularly polarized laser fields. Two ionization processes were considered. The first is resonance excitation. For H_2^+, the ground state $1s\sigma_g$ was chosen as the initial state. We mainly studied the resonance excitation from the ground state $1s\sigma_g$ to the first excited state $2p\sigma_u$, the frequency of the laser pulse for $|\Delta E| = \left|I_{\mathrm{p_{e1}}} - I_{\mathrm{p_{A'}}}\right| = |0.65 - 1.08| = 0.43$ a.u. ($I_{\mathrm{p_{e1}}}$ is the energy of the first excited state, and $I_{\mathrm{p_{A'}}}$ is the energy of the ground state). The laser wavelength selected accordingly was

$\lambda = 100$ nm ($\omega = I_{p_{e1}} - I_{p_{A'}} \approx 0.455$ a.u.). For HeH^{2+}, since the first excited state $2p\sigma$ is located at the equilibrium nuclear distance $R = 3.89$ a.u., it is relatively stable and has an average lifetime of 4 ns.[40] This is sufficient to ionize electrons from both the ground and excited states.[30] So, the first excited state $2p\sigma$ was chosen as the initial state. We investigate the resonance excitation from the first excited state $2p\sigma$ to the second excited state $2p\pi$, the frequency of the laser pulse for $|\Delta E| = |I_{p_{e1}} - I_{p_{A'}}| = |0.74 - 1.03| = 0.29$ a.u. ($I_{p_{e1}}$ for the second excited state energy, $I_{p_{A'}}$ is the first excited state (initial state) of energy). The laser wavelength selected accordingly is $\lambda = 150$ nm ($\omega = I_{p_{e1}} - I_{p_{A'}} \approx 0.3$ a.u.). The second is direct ionization. For both H_2^+ and HeH^{2+}, laser wavelength of $\lambda = 30$ nm ($\omega = 1.52$ a.u.) is selected, $\omega > I_p$. For H_2^+ and HeH^{2+}, the two ionization processes and the initial wave function densities of the selected electronic states are shown schematically in Fig. 1.

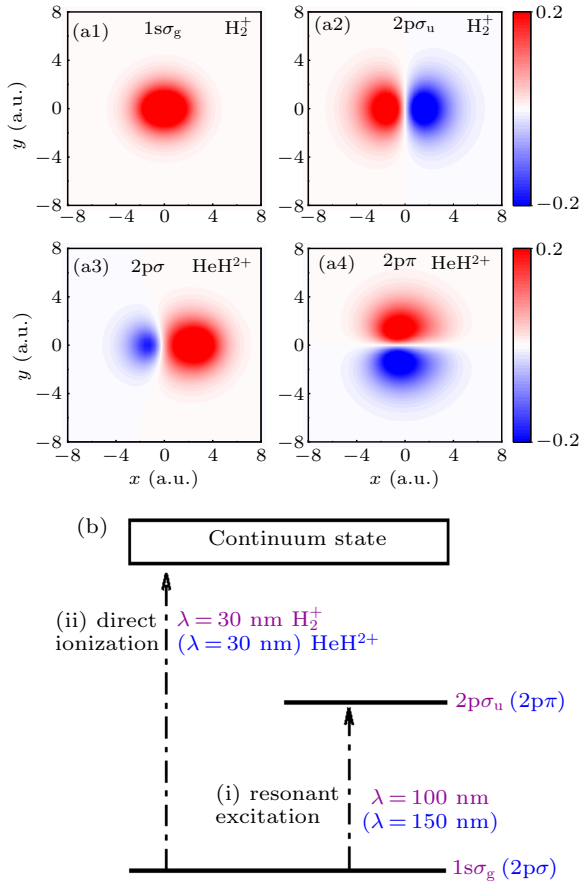


Fig. 1. (a1) and (a2) The densities of the initial wave function of ground state $1s\sigma_g$ of H_2^+ and the first excited state $2p\sigma_u$. (a3) and (a4) The initial wave function density of the first excited state $2p\sigma$ and the second excited state $2p\pi$ of HeH^{2+}. (b) Two ionization mechanisms are designed for calculation: (i) resonance excitation and (ii) direct ionization.

We investigated the PMDs and PADs of H_2^+ and HeH^{2+} in a circularly polarized laser field using different ionization mechanisms. The momentum distributions of H_2^+ and HeH^{2+} under the two ionization mechanisms were simulated at laser intensities $I_0 = 5\times10^{13}$ W/cm^2, 8×10^{13} W/cm^2, 1×10^{14} W/cm^2. From Figs. 2(a1)–2(a3) and 2(c1)–2(c3), it can be concluded that the PMDs of H_2^+ and HeH^{2+} in the y direction increase gradually with increasing intensity under both ionization conditions. For H_2^+, the PMDs (Figs. 2(b1)–2(b3)) present a two-lobe structure under (ii). However, under scenario (i), the PMDs in Figs. 2(a1)–2(a3) present a four-lobe structure. For HeH^{2+} in Figs. 2(d1)–2(d3) , the PMDs exhibit a six-lobe structure with (ii). Nevertheless, under scenario (i) in Figs. 2(c1)–2(c3), the PMDs become a four-lobe asymmetric structure. Under scenario (i) in Figs. 2(c1)–2(c3), the asymmetry of the PMDs gradually increased with increasing laser intensity. The above phenomena can be elucidated by the two-center interference and ultra-fast ionization model of molecules[24,41,44] as follows.

(i) Resonance excitation

For H_2^+, the pulse frequency $\omega = 0.455$ a.u., leads to a $1s\sigma_g$–$2p\sigma_u$ resonant excitation. Since the laser frequency is close to the frequency of two-photon ionization, it is believed that the main mechanism was two-photon ionization on the PMDs of H_2^+. In the two-photon ionization process, the transition amplitude can be expressed as

$$\begin{aligned} \boldsymbol{A} &\propto \langle\psi_c|\boldsymbol{r}\cdot\boldsymbol{E}|\psi_n\rangle\langle\psi_n|\boldsymbol{r}\cdot\boldsymbol{E}|\psi_0\rangle \\ &\sim (dx_1\cos\theta + dy_1\sin\theta)(dx_2\cos\theta + dy_2\sin\theta) \\ &\sim dx_1dx_2\cos^2\theta + dy_1dx_2\sin\theta\cos\theta \\ &\quad + dx_1dy_2\cos\theta\sin\theta + dy_1dy_2\sin^2\theta, \end{aligned} \tag{9}$$

$$\boldsymbol{A}_x \sim dx_1dx_2\cos^2\theta + dx_1dy_2\cos\theta\sin\theta, \tag{10}$$

$$\boldsymbol{A}_y \sim dy_1dx_2\sin\theta\cos\theta + dy_1dy_2\sin^2\theta, \tag{10}$$

where the ejection angle between the position of the electron $\boldsymbol{r}$ and the laser field is denoted by θ. The initial, intermediate, and continuous states are denoted as $|\psi_0\rangle$, $|\psi_n\rangle$, and $|\psi_c\rangle$, respectively. The total distribution is the sum of the square modulus of the transition amplitudes in the x and y directions and the interference term.

$$|A|^2 = |A_x|^2 + |A_y|^2 + A^{(x,y)}, \tag{11}$$

$$\begin{aligned} A^{(x,y)} &= A_x{}^*A_y + A_xA_y{}^* \\ &\sim \sin\theta\cos^3\theta + \cos^2\theta\sin^2\theta \\ &\quad + \sin^2\theta\cos^2\theta + \sin^3\theta\cos\theta. \end{aligned} \tag{12}$$

The angular range of θ is considered to be from $-\pi$ to π. Thus, $\sin\theta = -\sin(-\theta)$, $\cos\theta = \cos(-\theta)$, where the interference term is

$$\begin{aligned} A^{(x,y)} &\sim (-\sin\theta\cos^3\theta) + \cos^2\theta\sin^2\theta \\ &\quad + \sin^2\theta\cos^2\theta + (-\sin^3\theta\cos\theta). \end{aligned} \tag{13}$$

The calculated results of the PADs in Fig. 3(a) predicted by Eq. (13) are also in good agreement with the TDSE in Figs. 2(a1)–2(a3), showing a four-lobe structure, and the maximum values were distributed at 135° and 315°. Therefore, in scenario (i), two-photon ionization plays a dominant role in the PMDs in H_2^+.

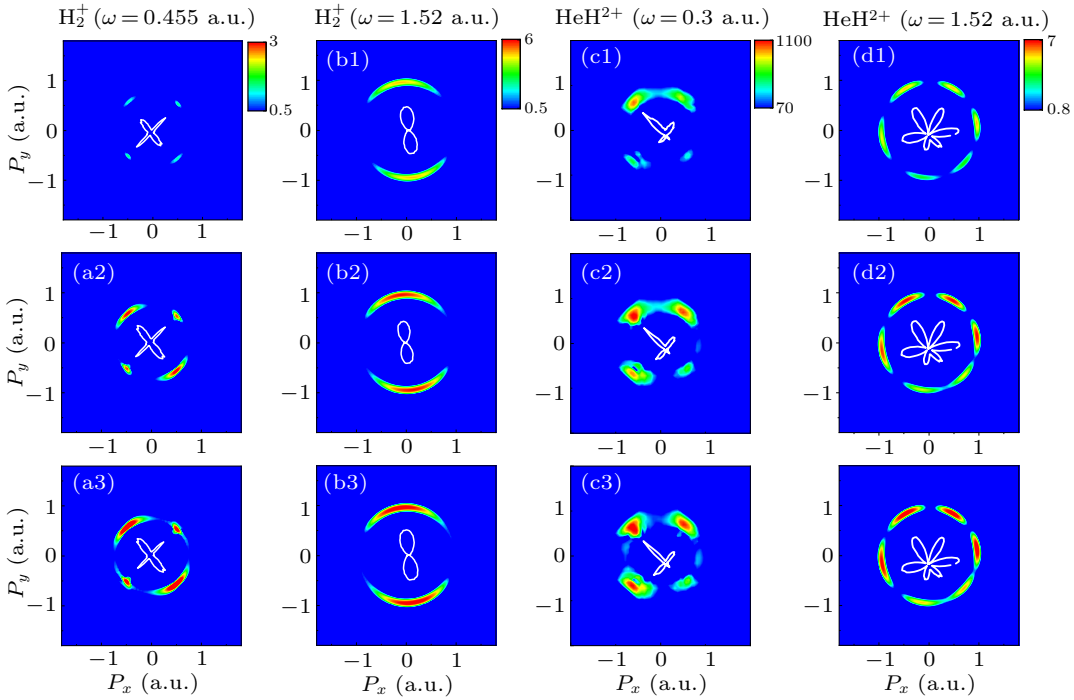


Fig. 2. (a1)–(a3) and (b1)–(b3) PMDs and PADs of H_2^+ in resonance excitation ($\omega = 0.455$ a.u.) and direct ionization ($\omega = 1.52$ a.u.) with laser intensity, respectively. (c1)–(c3) and (d1)–(d3) PMDs and PADs of HeH^{2+} in resonance excitation ($\omega = 0.3$ a.u.) and direct ionization ($\omega = 1.52$ a.u.). From top to bottom, the laser intensity was set to $I_0 = 5\times10^{13}$ W/cm^2, 8×10^{13} W/cm^2, and 1×10^{14} W/cm^2.

For HeH^{2+}, the pulse frequency $\omega = 0.3$ a.u. leads to a $2p\sigma$–$2p\pi$ resonant excitation. Since the laser frequency we selected was similar to the frequency of three-photon ionization, it is believed that the main mechanism was three-photon ionization on the PMDs of HeH^{2+}. In the three-photon ionization process, the transition amplitude is

$$\begin{aligned} \boldsymbol{A} &\propto \langle\psi_c|\boldsymbol{r}\cdot\boldsymbol{E}_x|\psi_m\rangle\langle\psi_m|\boldsymbol{r}\cdot\boldsymbol{E}_x|\psi_n\rangle\langle\psi_n|\boldsymbol{r}\cdot\boldsymbol{E}_x|\psi_0\rangle \\ &\sim (dx_1\cos\theta + dy_1\sin\theta)(dx_2\cos\theta + dy_2\sin\theta) \\ &\quad\times(dx_3\cos\theta + dy_3\sin\theta), \end{aligned} \tag{14}$$

$$\begin{aligned} \boldsymbol{A}_x &\sim dx_1dx_2dx_3\cos^3\theta + dx_1dy_2dx_3\cos^2\theta\sin\theta \\ &\quad + dx_1dx_2dy_3\cos^2\theta\sin\theta + dx_1dy_2dy_3\cos\theta\sin^2\theta, \\ \boldsymbol{A}_y &\sim dy_1dx_2dx_3\sin\theta\cos^2\theta + dy_1dy_2dx_3\sin^2\theta\cos\theta \\ &\quad + dy_1dx_2dy_3\sin^2\theta\cos\theta + dy_1dy_2dy_3\sin^3\theta, \end{aligned} \tag{15}$$

where the ejection angle between the position of the electron $\boldsymbol{r}$ and the laser field, is denoted by θ. $|\psi_0\rangle$ is the initial wave function, $|\psi_m\rangle$ and $|\psi_n\rangle$ are the intermediate state wave functions, and $|\psi_c\rangle$ is the wave function of the continuous state. The total distribution is the modulus square of the transition amplitudes in the x- and y-directions plus the interference term

$$|A|^2 = |A_x|^2 + |A_y|^2 + A^{(x,y)}, \tag{16}$$

$$\begin{aligned} A^{(x,y)} &= A_x{}^*A_y + A_xA_y{}^* \\ &\sim \sin\theta\cos^5\theta + \sin^2\theta\cos^4\theta + \sin^3\theta\cos^3\theta \\ &\quad + \cos^2\theta\sin^4\theta + \cos\theta\sin^5\theta. \end{aligned} \tag{17}$$

The angular range of θ is considered to be from $-\pi$ to π. Thus, $\sin\theta = -\sin(-\theta)$, $\cos\theta = \cos(-\theta)$, where the interference term is

$$\begin{aligned} A^{(x,y)} &\sim (-\sin\theta\cos^5\theta) + \sin^2\theta\cos^4\theta + (-\sin^3\theta\cos^3\theta) \\ &\quad + \cos^2\theta\sin^4\theta + (-\cos\theta\sin^5\theta). \end{aligned} \tag{18}$$

The calculated results of the PADs in Fig. 3(c) predicted by Eq. (18) and TDSE in Figs. 2(c1)–2(c3) both showed a four-lobe structure. However, the intensity was not consistent with that of the PADs. Because the molecular Coulomb potential is not included in the ultrafast ionization model, which is a simplified two-center model, the intensity of the anticipated findings is incompatible with the results of the TDSE simulation. Thus, the PMDs of HeH^{2+} are dominated by three-photon ionization in scenario (i).

(ii) Direct ionization

For H_2^+, the interference term can be obtained from equation (A.3) in Ref. [27]

$$A_{\sigma_g}^{(x,y)} \propto 2\cos^2(\boldsymbol{p}\cdot\boldsymbol{R}/2)\psi^2{}_{1s}(|\boldsymbol{p}|). \tag{19}$$

The calculated results of the PADs in Fig. 3(b) predicted by Eq. (19) were also in good agreement with those of TDSE (Fig. 2), both of which showed a two-lobe structure, and the maximum values were distributed at 90° and 270°. Therefore, two-center interference plays a dominant role in the PMDs of H_2^+ under scenario (ii). Figure 2(b3) shows the results in a CP laser pulse (30 nm, 1×10^{14} W/cm^2), which is similar to the experimental observation findings in a CP laser pulse (800 nm, 6×10^{14} W/cm^2) in Fig. 1(e) in Ref. [42]. Due to the non-spherical Coulomb potential and the laser field's helicity (which is consistent with previous experimental studies[42,43]), the calculated PMDs are primarily distributed along the y-axis

and have a small angle of deflection, the direction of which coincides with the laser field's rotational direction.[41,42]

For HeH^{2+}, the initial coordinate space wave function takes the following form:

$$\psi_{2p}(\boldsymbol{r}) = \psi_{2p}(\boldsymbol{r} - \boldsymbol{R}/5) + \psi_{2p}(\boldsymbol{r} + 4\boldsymbol{R}/5). \tag{20}$$

In momentum space, the initial wave function can be expressed as follows:

$$\phi(p) = \left(\frac{1}{\sqrt{2\pi}}\right)^3 \int \mathrm{e}^{-\mathrm{i}(\boldsymbol{P}+\boldsymbol{F})\cdot\boldsymbol{r}} \psi_{2p}(r)\,\mathrm{d}r. \tag{21}$$

In our calculation, because of $U_p \leq I_p, F \leq p$, it can be obtained that

$$\phi(p) \propto \left(\frac{1}{\sqrt{2\pi}}\right)^3 \int \mathrm{e}^{-\mathrm{i}\boldsymbol{P}\cdot\boldsymbol{r}} \psi_{2p}(r)\,\mathrm{d}r. \tag{22}$$

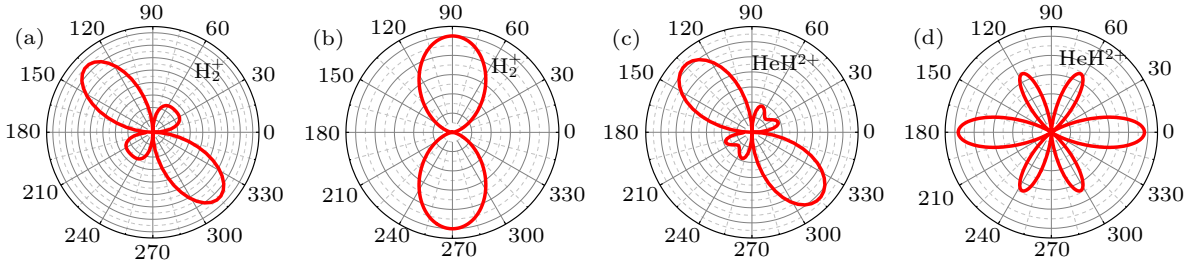


Fig. 3. The PADs of (a) H_2^+ and (c) HeH^{2+} predicted by Eqs. (13) and (18) under resonance excitation, and the PADs of (b) H_2^+ and (d) HeH^{2+} predicted by Eqs. (19) and (27) under direct ionization.

By substituting Eq. (20) into the above equation, it can be deduced that

$$\phi(p) \propto \mathrm{e}^{-\mathrm{i}\boldsymbol{P}\cdot\frac{\boldsymbol{R}}{5}} + \mathrm{e}^{\mathrm{i}\boldsymbol{P}\cdot\frac{4\boldsymbol{R}}{5}}. \tag{23}$$

Finally, the transition amplitudes of HeH^{2+} molecular ions in the x and y directions are

$$\begin{aligned} A_x \propto\ & \frac{1}{\sqrt{2}} c^{(x)} E_{x0}(\varepsilon) \frac{1}{\sqrt{1+\varepsilon^2}} \cos(\alpha) \\ & \times \left(\mathrm{e}^{-\mathrm{i}\boldsymbol{P}\cdot\frac{\boldsymbol{R}}{5}} + \mathrm{e}^{\mathrm{i}\boldsymbol{P}\cdot\frac{4\boldsymbol{R}}{5}}\right) \varphi(p), \end{aligned} \tag{24}$$

$$\begin{aligned} A_y \propto\ & \frac{1}{\sqrt{2}} c^{(y)} E_{y0}(\varepsilon) \frac{1}{\sqrt{1+\varepsilon^2}} \sin(\alpha) \\ & \times \left(\mathrm{e}^{-\mathrm{i}\boldsymbol{P}\cdot\frac{\boldsymbol{R}}{5}} + \mathrm{e}^{\mathrm{i}\boldsymbol{P}\cdot\frac{4\boldsymbol{R}}{5}}\right) \varphi(p), \end{aligned} \tag{25}$$

where the ionization probabilities in x and y directions are denoted by $c^{(x)}$ and $c^{(y)}$.

The square modulus of the x- and y-direction transition amplitudes plus the interference term equals the total distribution

$$|A|^2 = |A_x|^2 + |A_y|^2 + A^{(x,y)}. \tag{26}$$

Then, the modulus of the transition amplitude in the x direction can be written as

$$\begin{aligned} |A_x|^2 \propto\ & \frac{1}{2}\left(c^{(x)}\right)^2 E^2{}_{x0}(\varepsilon) \frac{1}{1+\varepsilon^2} \cos^2(\alpha) \\ & \times \left[2 + 2\cos(\boldsymbol{P}\cdot\boldsymbol{R})\right] \varphi^2(p). \end{aligned} \tag{27}$$

The PADs in Fig. 3(d) predicted by Eq. (27) are consistent with the calculated results of the TDSE in Figs. 2(d1)–2(d3), both of which show a six-lobe structure. Therefore, in scenario (ii), the modulus of the transition amplitude in the x-direction played a dominant role in the PMDs of HeH^{2+}. Moreover, in scenario (ii), the PMDs of H_2^+ and HeH^{2+} are dominated by the two-center interference model.

In order to further investigate the causes of the momentum distributions produced by H_2^+ and HeH^{2+} in scenario (i), the time-dependent populations of H_2^+ and HeH^{2+} are presented in Fig. 4. It can be observed that at the end of the laser pulse, for H_2^+, the sum of the population of the ground state and excited state is 0.95; for HeH^{2+}, the sum of the population of the ground state and excited state is 0.4, which means that the ionization of HeH^{2+} is much stronger than that of H_2^+ at the end of the laser pulse. Thus, the intensity of the PMD for H_2^+ should be lower than that for HeH^{2+}, which is in agreement with Figs. 2(a) and 2(c).

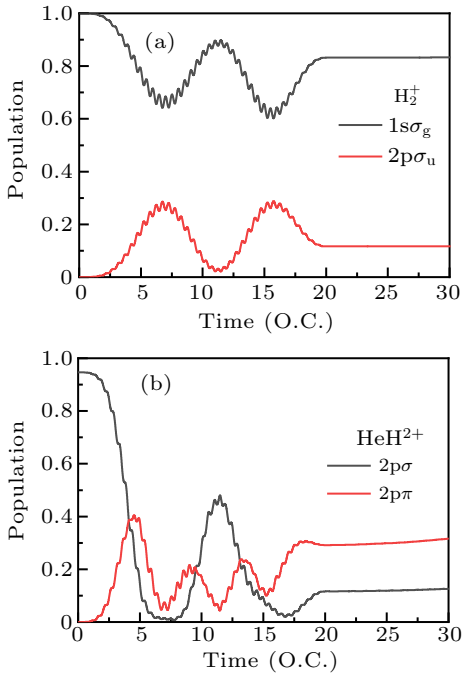


Fig. 4. (a) The time-dependent population of the ground state ($1s\sigma_g$) and the first excited state ($2p\sigma_u$) of H_2^+ in the scenario of resonance excitation. (b) The time-dependent population of the first excited state ($2p\sigma$) and the second excited state ($2p\pi$) of HeH^{2+} in the scenario of resonance excitation.

4. Conclusion

The photoionization of symmetric (H_2^+) and asymmetric (HeH^{2+}) molecular ions in a CP laser field was theoretically investigated. Under the two designed ionization conditions, our results show that the PMDs of H_2^+ and HeH^{2+} in the y-direction were gradually enhanced with increasing intensity. In the direct ionization scenario, the PMDs of H_2^+ and HeH^{2+} are dominated by the two-center interference model. In the resonance excitation scenario, the PMDs of both H_2^+ and HeH^{2+} exhibit a four-petal structure, two-photon ionization takes a leading role in the PMDs of H_2^+, and the PMDs of HeH^{2+} are dominated by three-photon ionization. In addition, we found that the PMDs of HeH^{2+} exhibited greater asymmetry than that of H_2^+ in the resonance excitation scenario and the intensity of the PMDs for HeH^{2+} was higher than that of H_2^+. This is related to the fact that at the end of the laser pulse the ionization of HeH^{2+} is much stronger than that of H_2^+. The time evolution of the electron population was used to explain this phenomenon in detail. In the resonance excitation scenario, the PMDs and ionization of molecular ions are stronger, which means that more abundant molecular dynamics information can be obtained. It is also helpful to investigate the internal motion and reaction dynamics of molecules.

Acknowledgements

Project supported by the Natural Science Foundation of Jilin Province (Grant No. 20220101010JC) and the National Natural Science Foundation of China (Grant No. 12074146).

References

[1] Agostini P, Fabre F, Mainfray G, Petite G and Rahman N K 1979 *Phys. Rev. Lett.* **42** 1127
[2] Li W K , Lei Y, Li X, Yang T, Du M, Jiang Y, Li J L, Luo S Z, Liu A H, He L H, Ma P, Zhang D D and Ding D J 2021 *Chin. Phys. Lett.* **38** 053202
[3] Meng C S, Lü Z H, Wang X W, Zhang D W, Zhao Z X and Yuan J M 2022 *Chin. Phys. Lett.* **39** 113701
[4] Yang Q, Leng J, Wang Y H, Sun Y N, Du H B, Zhang D D, Song L L, He L H and Liu F C 2022 *Chin. Phys. Lett.* **39** 023301
[5] Corkum P B, Burnett N H and Brunel F 1989 *Phys. Rev. Lett.* **62** 1259
[6] Watanabe S, Kondo K, Nabekawa Y, Sagisaka A and Kobayashi Y 1994 *Phys. Rev. Lett.* **73** 2692
[7] Peatross J and Meyerhofer D D 1995 *Phys. Rev. A* **52** 3976
[8] Miyazaki K and Takada H 1995 *Phys. Rev. A* **52** 3007
[9] Krausz F and Ivanov M 2009 *Rev. Mod. Phys.* **81** 163
[10] Chang Z H and Corkum P B 2010 *J. Opt. Soc. Am. B* **27** B9
[11] Paul P M, Toma E S, Breger P, Mullot G, Auge F, Balcou PH, Muller H G and Agostini P 2001 *Science* **292** 1689
[12] Baltuska A, Udem Th, Uiberacker M, Hentschel M, Goulielmakis E, Gohle Ch, Holzwarth R, Yakovlev V S, Scrinzi A, Hansch T W and Krausz F 2003 *Nature* **421** 611
[13] Corkum P B 2013 *Attosecond Physics* (Springer Series in Optical Sciences)
[14] Kfir O, Grychtol P, Turgut E, Knut R, Zusin D, Fleischer A, Bordo E, Fan T, Popmintchev D, Popmintchev T and others 2016 *J. Phys. B: At. Mol. Opt. Phys.* **49** 123501
[15] Zhang X F, Li L, Zhu X S, Liu X, Zhang Q B, Lan P F and Lu P X 2016 *Phys. Rev. A* **94** 053408
[16] Milošević D B 2016 *Phys. Rev. A* **93** 051402
[17] Bandrauk A D, Mauger F and Yuan K J 2016 *J. Phys. B: At. Mol. Opt. Phys.* **49** 23LT01
[18] Reich D M and Madsen L B 2016 *Phys. Rev. A* **93** 043411
[19] Zhang C P and Miao X Y 2023 *Chin. Phys. Lett.* **40** 124201
[20] Niikura H, Villeneuve D M and Corkum P B 2005 *Phys. Rev. Lett.* **94** 083003
[21] Shao H C and Starace A F 2010 *Phys. Rev. Lett.* **105** 263201
[22] Meckel M, Comtois D, Zeidler D, Staudte A, Pavicic D, Bandulet H C, Pepin H, Kieffer J C, Dorner R, Villeneuve D M and Corkum P B 2008 *Science* **320** 1478
[23] Yuan K J, Chelkowski S and Bandrauk A D 2015 *Chem. Phys. Lett.* **638** 173
[24] Zhang H D, Ben S, Xu T T, Song K L, Tian Y R, Xu Q Y, Zhang S Q, Guo J and Liu X S 2018 *Phys. Rev. A* **98** 013422
[25] Li Y, Qin M Y, Zhu X S, Zhang Q B, Lan P F and Lu P X 2015 *Opt. Express* **23** 10687
[26] Yuan K J, Lu H Z and Bandrauk A D 2011 *Phys. Rev. A* **83** 043418
[27] Yuan K J and Bandrauk A D 2012 *J. Phys. B: At. Mol. Opt. Phys.* **45** 105601
[28] Hatsui T, Nagasono M and Kosugi N 2004 *J. Electron. Spectrosc. Relat. Phenom.* **137** 435
[29] Hollstein M and Rohringer N 2019 *Phys. Rev. A* **99** 013425
[30] Chen Y and Zhang B 2012 *Phys. Rev. A* **86** 023415
[31] Miao X Y and Du H N 2013 *Phys. Rev. A* **87** 053403
[32] Xu Q Y, Yang Z J, He Y L, Gao F Y, Lu H Z and Guo J 2021 *Opt. Express* **29** 32312
[33] Guan X, Secor E B, DuToit R C and Bartschat K 2012 *Phys. Rev. A* **86** 053425
[34] Bian X B and Bandrauk A D 2011 *Phys. Rev. A* **83** 023414
[35] Campos J A, Nascimento D L, Cavalcante D T, Fonseca A L and Numesa A O 2006 *Int. J. Quantum Chem.* **106** 2587
[36] Yuan K J, Chelkowski S and Bandrauk A D 2014 *Chem. Phys. Lett.* **592** 334
[37] Wind H 1965 *J. Chem. Phys.* **42** 2371
[38] Bandrauk A D and Shen H 1993 *J. Chem. Phys.* **99** 1185
[39] Bandrauk A D and Lu H 2013 *J. Theor. Comput. Chem.* **12** 1340001
[40] Ben-Itzhak I, Gertner I, Heber O and Rosner B 1993 *Phys. Rev. Lett.* **71** 1347
[41] Zuo T, Bandrauk A D and Corkum P B 1996 *Chem. Phys. Lett.* **259** 313
[42] Odenweller M, Takemoto N, Vredenborg A, Cole K, Pahl K, Titze J, Schmidt L P, Jahnke T, Dorner R and Becker A 2011 *Phys. Rev. Lett.* **107** 143004
[43] Akoury D, Kreidi K, Jahnke T, *et al.* 2007 *Science* **318** 949
[44] Ansari Z, Böttcher M, Manschwetus B, *et al.* 2008 *New J. Phys.* **10** 093027